Evaluation of the economic feasibility of a two-stage gasification system for hydrogen, liquid fuels and energy production from residues

Hannah O. Kargbo[1], Kok Siew Ng[2], Anh N. Phan[1,*]

[1]School of Engineering, Newcastle University, Newcastle upon Tyne NE1 7RU

[2] Department of Engineering Science, University of Oxford, Parks Road, Oxford OX1 3PJ.

Abstract

Although two-stage gasifier design offers a number of advantages i.e., producing high-quality gas (high H_2 content, low CO_2 and other impurities) and tolerating high degree of heterogeneity of feedstock, its economic feasibility is yet to be evaluated. In this study, a techno-economic assessment is fully conducted to assess the economic feasibility of a two-stage gasification system for three routes: hydrogen production, liquid fuels via Fischer-Tropsch synthesis, and electricity production. For a two-stage gasification of 20 years at a plant size of 1000 dry t/d, the total capital investment for hydrogen, FT-liquid and electricity production are US $214.8 million, US $345.5million and US $307 million with operation costs of US $35.6 million/y, US $62.2 million/y and US $48.6 million/y, respectively. The minimum selling price for hydrogen (pressured at 70 bar) and liquid fuel is similar to that from fossil fuels (US $1.59/kg for H_2 and US $1,109/m^3 for liquid fuel) whereas for electricity (US $ 0.09 /kWh), it is around half of the current electricity price from the grid in the UK. Comparing to conventional fluidised bed gasification for the same feedstock, around 25% reduction was achieved for either hydrogen or liquid fuel production but only around 10% reduction was for electricity. The results also show that the economics of the system can be improved further by (35-40%) if the cost of feedstock is reduced (30-50%) at large-scale production facility (≥2000 dry t/d).

Keywords: two-stage gasification, hydrogen, gasification-to-liquid fuels, gasification-to-hydrogen, syngas, economic of scales

*Corresponding author's email: anh.phan@newcastle.ac.uk

1.0 Introduction

Concerns over negative impact associated with the usage of fossil fuels and the depletion of finite natural resources have led to increasing focus on deploying alternative renewable and sustainable resources. The transportation sector heavily relies on petroleum-based sources (~90% of transportation fuel used worldwide), contributing nearly one third of total greenhouse gas emissions in the UK and 28% worldwide (Department for Business, 2020; EPA, 2020). To achieve the net zero emission target by 2050 in the UK and EU, it is importance to increase the uptake of alternative renewable fuels for transportation, heat and electricity. The continue increasing the world population

(average of 1% per annum) and GDP has led to an increase in energy demand. Therefore, alternative and sustainable energy sources are vital.

Although renewable energies such as solar and wind have enormous potential for producing clean energy in terms of heat and electricity (Zuo et al., 2019; Zuo et al., 2021), these energy sources are intermittent and therefore need to be integrated into energy storage systems. Graphene, a two-dimensional allotrope of carbon-based materials with a high specific surface area, excellent chemical stability, and exceptional electrical properties, has been shown as an ideal candidate for energy conversion and storage devices (Zhao et al., 2019). Biomass waste and residues is abundant, cheap, and renewable which can be converted into a number of energy vectors. Gasification, a thermochemical process occurring under a temperature of >750℃ in oxidising environment (limited air/oxygen, CO_2, steam or combination), is a promising approach to convert biomass into syngas (a mixture of H_2 and CO) , which can be combusted in gas combustion engines for energy, separated for hydrogen or further processed for chemicals and liquid fuels (Ng et al., 2014). However, biomass gasification has still encountered some challenges due to high degree of heterogeneity, high volatile content (3-4 times higher than coal) and slagging issues (Ku et al., 2019; Prasertcharoensuk et al., 2019; Riaza et al., 2019)). The rapid release of volatile content in biomass as soon as it is heated up to 250^{o}C, is prone to tar formation (i.e. high molecular weight molecules condensing when cooled down at temperatures below 250^{o}C (Harb et al., 2020)). Furthermore, low H_2/CO ratios (0.8-1), high CO_2 (25%), high tar contents (20-30 g/m^3) (Lu et al., 2019) in the producer gas require cleaning and conditioning before it can be used for hydrogen, chemicals or liquid fuels production. Current biomass gasification technology produces low quality gas, therefore, it is used mainly for heat and electricity purposes. This is because the cleaning, conditioning and purification of the gas are costly (Simell et al., 2014), accounting up to 12–15% of production costs and 11-18% of capital costs (Kargbo et al., 2021). A significant amount of carbon (8.28%) and hydrogen (4%) in feedstock remains in tar (Tan et al., 2020) that needs to be removed, therefore reducing the overall efficiency (~ 15-20%) of biomass gasification. Tar treatment (removal and/or cracking either *in situ* or *ex situ*) have been carried out extensively as evidenced by a number of review papers (Anis and Zainal, 2011; Devi et al., 2003; Rios et al., 2018; Shen and Yoshikawa, 2013). A commercial technique for tar removal is to use of bio-oil, i.e. rapeseed methyl ester scrubber (Paethanom et al., 2012) alongside others at research and pilot stages such as woodchip bed or char and mop fan to capture tar from syngas (Hai et al., 2019; Ravenni et al., 2019), chemical looping for *in situ* tar removal (Zeng et al., 2019), and biochar-based nanocatalysts for tar cracking/reforming (Guo et al., 2020).

Common gasifiers include fluidized bed, fixed bed and entrained flow gasifiers. Although fluidized bed gasifiers exhibits good mass and heat transfer (Broer and Peterson, 2019), it requires highly

homogeneous feedstock with moisture content below 20% and small size (~20mm) (Rasmussen and Aryal, 2020). Fixed bed gasifiers, particularly downdraft types, are simple and can accommodate feedstock with high ash content and suitable for small-scale production (10-20 t/d). The producer gas from both fluidized and fixed bed gasifiers contains high tar content (30-70 g/m^3) and low H_2 content (20-40 mol%), high CO_2 content (20-25 mol%). The properties of the producer gas are much lower than those required for Fischer-Tropsch (FT) synthesis (H_2/CO ~2, tar <1.5mg/m^3) and CO_2 <5%) (Zhao, Xianhui et al., 2019) and for methanol production (H_2/CO_2~3, tar < 1.5mg/m^3, particulate <0.1ppm and CO_2 4-8%) (Dalena et al., 2018)). Although entrained flow gasifier produces the producer gas with low tar (2-3g/m^3), high H_2/CO (2.4) and low CO_2 (10-15%), its adaptability to feedstock is poor, therefore limited in its applications. Plasma gasification has also been explored for producer gas with low tar content (Kuo et al., 2020; Saleem et al., 2019). However, operating the plasma gasifier at high temperatures (few thousand degrees) requires specialised equipment and complex cooling systems led to limited applications (mainly for hazardous waste) (Ramos et al., 2020). Supercritical water gasification of biomass (300 bar and 500°C- 700°C (Chen et al., 2019a)) can be applied for hydrogen production via the water-gas shift reaction and can produce syngas with low tar content and high gasification efficiency (Chen et al., 2019b). A separated approach i.e. a pre-treatment step such as pyrolysis and/or torrefaction of biomass to produce char (solid fuel) for gasification or co-gasification with coal was also studied (Kok Siew Ng and Sadhukhan, 2011). However, > 50% of biomass feedstock are transferred into the gas and liquid that are mainly used for heating only, therefore emitting CO_2 into the atmosphere. Moreover, the liquid derived from pyrolysis is thermally and chemically unstable e.g. solidifying when heated above 80˚C and polymerising during storage (Meng et al., 2015) because it has high oxygen content with more than hundreds of oxygenated compounds (Hu et al., 2016; Zhang et al., 2007), high viscosity and acidity. Therefore, two separate processes should be integrated into a one process (two-stage gasification) so that all elements in biomass feedstock can be fully converted into the high-quality syngas. In addition, the integrated two-stage gasification system offers other advantages such as utilising CO_2 released from pyrolysis as oxidising agent to react with volatiles (via dry reforming) and carbon in char fraction (via Boudouard reaction).

With more than 75% volatile content in biomass that rapidly releases in a temperature range of 250-650^{o}C, the devolatilisation step must be tightly controlled to improve the properties of the producer gas. Thus, the concept of a two-stage gasification, where the devolatilization and the gasification process occur in two separate zones, enables the gasification process to take place under optimised operational conditions within each zone. A number of two-stage gasifiers were installed and tested in both pilot and lab scales e.g. the two-stage 75 kWth Viking gasifier at the Danish Technical University (Henriksen et al., 2006), circulating fluidized bed gasifiers (Nielsen et al., 2005), a pilot-scale two-stage

air gasification in Korea (Jeong et al., 2020), a 5 t/d pilot plant in Denver, Colorado (E4Tech, 2009) and a 40 t/d circulating dual fluidised beds (FICFB) technology operated by REPOTEC in Güssing, Austria) (E4Tech, 2009).

Techno-economic analysis (TEA) is used to assess economic feasibility and scalability of emerging technologies. It assists businesses to identify the suitable end-product(s) and areas that need to be improved and optimised to ensure the profitability. Although two-stage gasification has proved a number of advantages over single-stage gasification, economic assessment has not been carried out to predict the feasibility as well as scale up opportunities for two-stage gasification. In contrast, techno-economic studies for single-stage biomass gasification for biofuel and hydrogen production have been carried out (Cardoso et al., 2019; Ng and Phan, 2021; Salkuyeh et al., 2018; Sara et al., 2016; Snehesh et al., 2017; Swanson et al., 2010). It is clear that a minimum selling price (MFSP) is up to 70% higher than that from fossil fuel due to downstream processes such as cleaning and purification of the producer gas and high costs of feedstock (contributing to 29%) (Salkuyeh et al., 2017, 2018). For decentralized small hydrogen production facilities (i.e. 100 kW_{th}), the MFSP of hydrogen is high (9.5 - 12.75 €/kg) (Sara et al., 2016) due to the costs of gas purification and conditioning processes. Advanced technologies e.g. steam gasification in dual fluidised beds and sorption enhanced reforming using fluidised beds of woody biomass still produce hydrogen at a cost 3.2 $/kg and 6.4 $/kg respectively (Bioenergy, 2018), which are 60%-80% higher than hydrogen from steam reforming of methane.

With the clear advantages of two-stage gasification in terms low tar and CO_2, high hydrogen content, techno-economic assessment is required to predict economy of scale and to commercialise the two-stage gasification (TSG) technology. Therefore, the aim of this work is to examine the economic feasibility of a two-stage biomass gasification system (using waste wood as feedstock) over a range of products: hydrogen, FT-liquid and electricity. Aspen plus simulation models for a two-stage biomass gasification system integrated with hydrogen/FT-liquid/electricity generation are established. The economic performance of the system is evaluated to identify the most economically attractive production route as well as the opportunities and barriers for process improvement. Consolidating the knowledge on this aspect helps identifying the opportunities and barriers in the development of this technology while enabling further optimisation work to be carried out.

2.0 Methodology

Figure 1 shows a flow diagram of the basic steps used for the techno-economic analysis for the three production routes (hydrogen, FT-liquid and electricity production). Flow diagrams were first developed based on literatures and the lab-scale two-stage gasifier developed at Newcastle

University. The downstream processing of the producer gas including operating conditions and composition for individual steps in the flow diagrams were adapted from others (Spath et al., 2005; Swanson et al., 2010). These were then used for constructing the process flowsheet and for sizing equipment. Cost of equipment was obtained via Aspen Plus activated economy and literature (Garcia-Peréz et al., 2020; Spath et al., 2005; Swanson et al., 2010). For the two-stage gasifier the cost for both zones (pyrolysis and gasification) was estimated separately and then sum-up to give the actual cost of a TSG reactor. The electricity consumption in each area of the plant was also obtained from Aspen Plus. After obtaining cost for each equipment, the information was used to calculate the capital investment and operating costs for each route (hydrogen, FT-liquid and electricity. A discounted cash flow rate of return analyses was obtained then the minimum fuel selling price/levelized cost of electricity (MFSP/LCOE) was calculated.

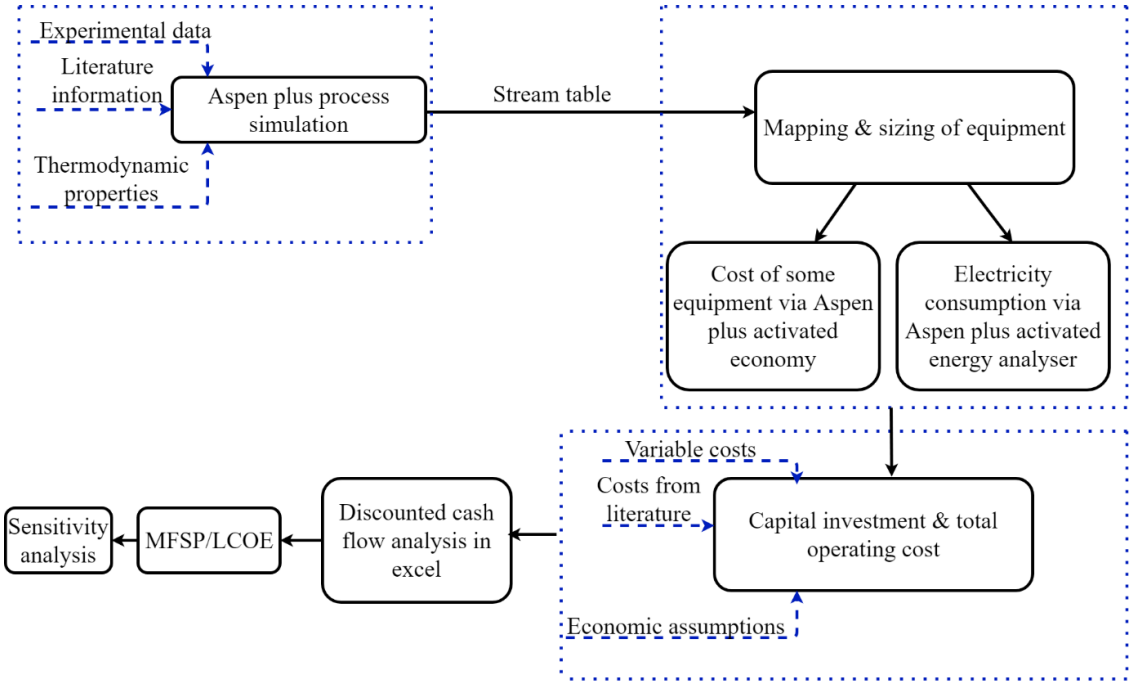

Figure 1: Flow diagram of the basic steps used for the techno-economic analysis

2.1 Process simulation and modelling

Thermodynamics equilibrium based on RGIBBS model was used to simulate the waste wood gasification process. the RGibbs model evaluates the chemical equilibrium constant for each reaction at a reactor temperature thereby giving an equilibrium gas composition. The biomass was first pyrolyzed at 900˚C in a Ryield reactor in which the product yields were specified based on our experimental results obtained from a lab-scale TSG. The products were then gasified at 1000°C and 1 bar (a RGIBBS reactor) with a known amount of steam. For the FTS process using a cobalt based catalyst, the syngas conversion was set at 0.95. A calculator block was formulated to calculate an alpha

(α) chain growth parameter using specified equations found by Song et al. (Song et al., 2004) . The FT products were specified as paraffins from C_1 through C_{20} and FT waxes are paraffins at C_{20}^+. The mole fraction of each hydrocarbon was calculated based on the calculated α value of 0.88 and the products distribution factor set at 0.90. The power generation process was simulated at a steady state condition (Zheng and Furimsky, 2003) using a syngas combustion turbine. The combustion turbine was operated at 1500°C. A detailed modelling process (including the Aspen plus blocks used for individual operation units with their operating conditions, mass/heat balances, flow sheet diagram and properties of waste wood feedstock) can be found in supplementary material A.

2.2 Economic analysis approach

The main assumptions used for the economic analysis together with the cost factors are given in Table 1. The total capital investment was estimated based on the total installed equipment cost (TIC), indirect and working capital costs. Equipment was sized based on mass flow in, residence time, heat requirements etc. prior to obtaining their costs. The capacities of the gasifier and dryer were used to estimate their cost using equation (1). The purchased costs of equipment were multiplied by a cost/installation factor ranging from 1.2 to 3.02 (Jones, 2015) to obtain the installed equipment cost. The chemical engineering plant cost index was used to convert all the cost to 2020 US dollars via equation (2). This cost estimation method is applicable for a conceptual design and has an expected accuracy of +/ -30% (Spath et al., 2005). A summary of the individual equipment costs for all three designs can be found in Table C1 in the supplementary material.

$$\text{New equipment cost} = \text{Old equipment cost} \times \left(\frac{\text{New capacity}}{\text{Old capacity}}\right)^{n} \text{(Sadhukhan et al., 2014)} \quad (1)$$

Where,

n: the scaling size factor (0.6-1 depending on the equipment).

$$C_{P} = C_{O} \times \frac{I_P}{I_O} \quad \text{(Sadhukhan et al., 2014)} \quad (2)$$

Where,

C_P = is the present cost

C_O = the original cost

I_P = the present index value

I_O = the original index value.

184

185 Table 1: General economic assumptions and cost factors (Swanson. et al., 2010)

A. Economic Parameters	
Financing (owner's equity)	100% (no money is borrowed from the bank to set up the business)
Internal rate of return	10%
Construction period	2.5 years with total capital investment spent at 8%, 60%, and 32% per year during years before operation (Swanson. et al., 2010)
Start-up time	0.5 years, where during this period, revenues, variable operating costs, and fixed operating costs are 50%, 75%, and 100% of normal, respectively.
Corporate tax	21%
Contingency	10% of total direct and indirect costs (TDIC)
Land purchase (LP)	6% of total purchased equipment cost
Feedstock cost (waste wood)	50 $/t (dry biomass) (Kargbo, Hannah et al., 2021) .
Plant availability (days per annum)	310
Hours per year	4,960
Plant capacity	1000 t/d (dry waste wood)
Plant life	20 years
B. Total Capital Investment (TCI)	
Total Purchased Equipment Cost (TPEC)	Literature (Garcia-Peréz et al., 2020; Spath et al., 2005; Swanson et al., 2010)
Total Installed Cost (TIC)	TPEC x Installation Factor
Indirect costs (IC)	89% of TPEC (Spath et al., 2005)
Total direct & indirect costs (TDIC)	TIC + IC + LP
Fixed capital investment (FCI)	TDIC + Contingency
Working capital (WC)	15% of FCI
Total capital investment (TCI)	FCI + WC
C. Fixed Operating Costs (FOC)	

	Maintenance	5% of IC
	Labour	Labour requirements, salary allocation and number of employees were obtained from (Spath et al., 2005) and scale to 1000 t /d of feedstock throughput. The total labour cost was estimated to be US$1.4 million, which is in accordance with the United States Bureau of Labour Statistics. Detail of the labour cost can be found in supplementary document B (Table B2)
	Laboratory cost	20% of labour cost
	Supervision	5% of labour cost
	Plant overheads	30% of labour cost
	Capital charges	5% of IC
	Insurance, tax and royalties	3% of IC
	Storage	1% of contingency
D. Other direct operating costs (ODOC)		
	Sales expense	2% of DPC
	General overheads	10% of DPC
	R&D	10% of DPC
E. Total operating Cost		
	Variable operating cost (VC)	From literature estimates (supplementary material, table B3)
	Total operating Cost	VC + FOC + ODOC

186

187 The MFSP is obtained using the equation (3) (Ng and Phan, 2021) .

188 $$\mathrm{MFSP} = \frac{(\mathrm{TOC}+\mathrm{ACC})}{\text{Annual plant yield}} \quad (3)$$

189 Where, *TOC* represent the total operating cost and *ACC* is the annualized capital cost. Annualized
190 capital cost was calculated using equation (4)(Ng and Martinez-Hernandez, 2020).

191 $$\text{Annualized capital cost} = \mathrm{TCI} * \mathrm{CRF} \quad (4)$$

192 Where, *TCI* is the total capital investment and *CRF (0.08)* is the capital recovery factor which has been
193 calculated using equation (5)(Ng and Martinez-Hernandez, 2020).

$$CRF = \frac{r(1+r)^n}{(1+r)^n - 1} \quad (5)$$

Where, r is the discounted rate which is 5% and n is the life span of the plant (20 years)

3.0 Results and Discussion

3.1 Process modelling

Figure 2 shows a simplified block flow diagram of TSG for three routes (a) hydrogen; (b) FT-liquid; and (c) electricity production. The composition and conditions for each stream in the flow diagram are tabulated in Table 2. A detailed design can be found in supplementary material A.

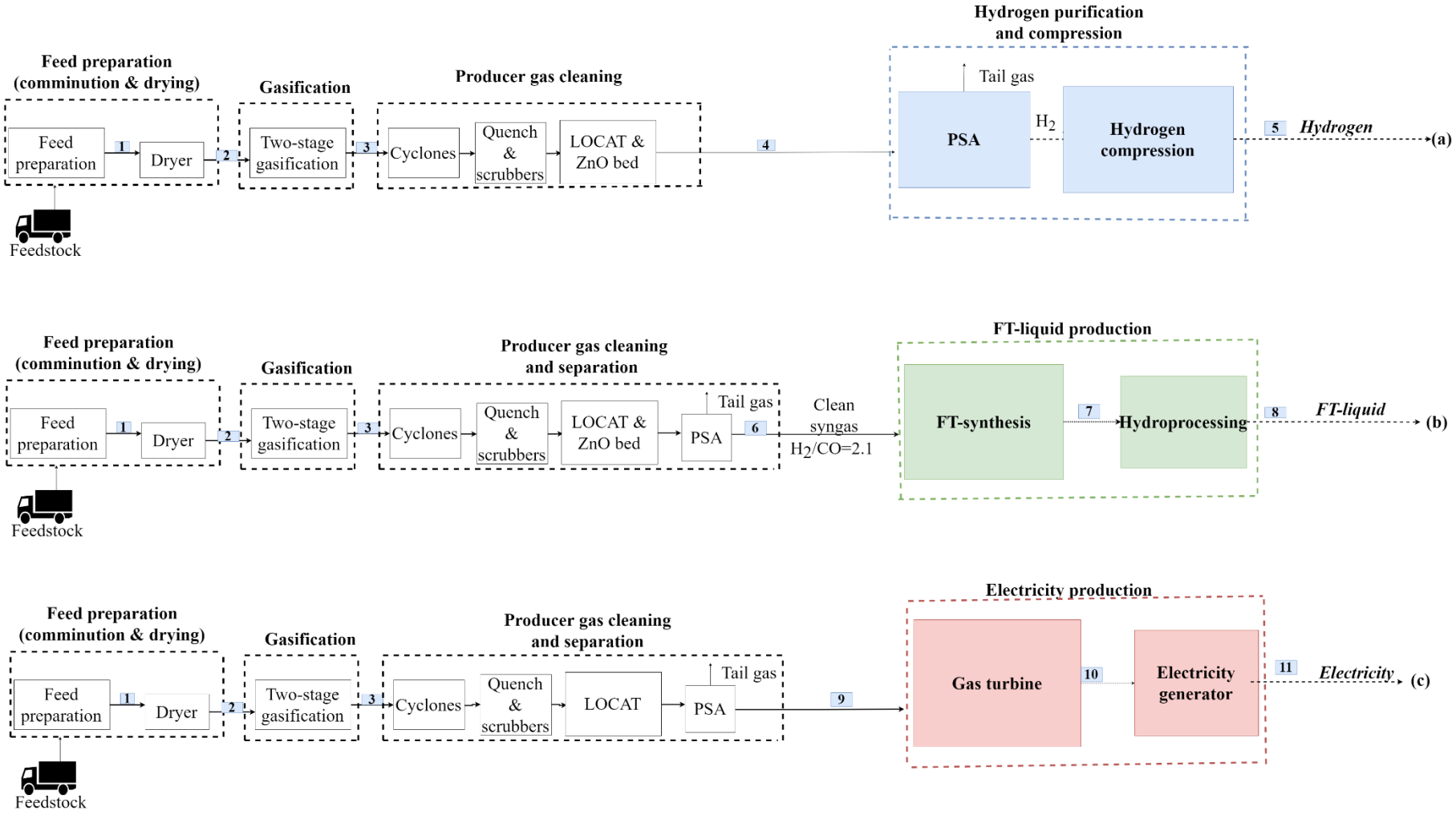

206

207

208 Figure 2: Block flow diagram of the integrated TSG for (a) hydrogen; (b) FT-liquid and (c) electricity production.

209 Table 2: Compositions and conditions for a 1000 t/day plant of TSG with (a) hydrogen; (b) FT-liquid ; and (c) electricity production.

Stream		**1**	**2**	**3**	**4**	**5**	**6**	**7**	**8**	**9**	**10**	**11**
Components	**Units**											
Temperature	°C	10	104	1000	43	41	43	200	24	43	1500	1500
Pressure	bar	1	1	1	25	70	25	25	23	25	1	1
Total mass Flow	kg/h	1000000	726000	404714	105521	73132	92398	369427	243856	92398	832	832
H_2	kg/h	0	0	75482	75482	73132	63958	7739	0	63958	0	0
CO	kg/h	0	0	10111	10111	0	28440	16064	0	28440	0	0
N_2	kg/h	0	0	7200	7200	0	0	0	0	0	0	0
CO_2	kg/h	0	0	15790	11567	0	0	0	0	0	690	690
H_2O	kg/h	300000	30000	294816	0	0	0	82382	0	0	22	22
H_2S	kg/h	0	0	123	0	0	0	0	0	0	0	0
NH_3	kg/h	0	0	9	0	0	0	0	0	0	0	0
CH_4	kg/h	0	0	1122	1122	0	0	173	0	0	120	120
C_2H_6	kg/h	0	0	12	12	0	0	19	0	0	0	0
C_2H_4	kg/h	0	0	14	14	0	0	0	0	0	0	0
C_2H_2	kg/h	0	0	16	6	0	0	0	0	0	0	0
C_6H_6	kg/h	0	0	12	7	0	0	50	0	0	0	0
Tar ($C_{10}H_8$)	kg/h	0	0	7	0	0	0	0	0	0	0	0
Char	kg/h	0	0	0	0	0	0	0	0	0	0	0
Biomass	kg/h	700000	696000	0	0	0	0	0	0	0	0	0

Waxes	kg/h	0	0	0	0	0	0	57000	0	0	0	0 210
C_5-C_{20}	kg/h	0	0	0	0	0	0	206000	243856	0	0	0

211

Feed preparation: waste wood feedstock is conveyed through a magnetic separator and screened to remove any metals. The feed leaving the magnetic separator is passed through a hammer mill crusher for size reduction to 1 cm (optimum size for high syngas yield) (Prasertcharoensuk et al., 2019). The stream 1 containing free metal 1cm cubes waste wood with moisture content of 30 wt% (wet basis) enters a rotary dryer modelled as an RStoic reactor (operated at 104℃, 1 bar and uses heated air at 100˚C as the drying medium) to reduce the moisture content to 10 wt%. The air from the dryer is sent to a cyclone and a baghouse filter to remove any particulates prior to release to the atmosphere.

Gasification: From the dryer (stream 2), the dried feed (at a mass flow rate of 726000kg/h) enters the TSG operated at the atmospheric pressure. Temperature is set at 900˚C for the first stage and 1000°C for the second stage. Steam (steam/carbon: 3.8 for the hydrogen production and 2.8 for the FT-liquid and electricity production routes) is injected into the second stage. In the TSG design, gasification-water gas shift and steam reforming are combined in one step. Therefore, there is no water gas shift unit operation included. This TSG configuration account for the high yield and quality syngas (Prasertcharoensuk et al., 2019) and thus reduced costs associated with syngas conditioning and tar cracking/reforming as oppose to a single-stage gasification system. A detailed modelling process can be found in supplementary material A.

Syngas cleaning and separation: Particulates present in the syngas are eliminated via cyclone separators followed by an electrostatic precipitator with a removal efficiency of 99% (Poškas et al., 2018). The syngas still contains some other contaminants such as H_2S, CO_2, ammonia, alkali metals, and tar etc. These contaminants are removed via cold gas cleaning technologies using amine scrubbers and a liquid phase oxidation (LO-CAT) process followed by a ZnO bed (Spath et al., 2005) (stream 4). The scrubbing system consists of a venturi scrubber and a quench chamber. Prior to the quench stage, the hot gases (1000˚C) are cooled to 150 ˚C with heat exchangers for heat recovery. Excess water from scrubbers were sent off site to a wastewater treatment facility and solids removed from the scrubbing process are also sent to a waste treatment facility. The LO-CAT is assumed to remove the sulphur to a concentration of about 10ppm, and the ZnO bed further reduces the sulphur content to less than 1ppm (Spath et al., 2005).For the electricity generation case, only LO-CAT is used as the requirement of sulphur in the syngas for electricity generation is around 20 ppm which can be met using LO-CAT system. After the cold gas cleaning, LOCAT and ZnO bed phase, the syngas passes through a pressure swing adsorption (PSA) unit were unreacted gases such as CO_2, CH_4, CO and other hydrocarbons are separated from the syngas prior to further downstream processes. Traces of water and condensed hydrocarbons must be removed prior to the gas entering the PSA to avoid damages of adsorbents (mixture of zeolite and activated carbon) in the PSA. To avoid the occurrence of the above situation a knockout drum with a mist eliminator was included in the design prior to the PSA. Moreover, the efficiency of the PSA can also be affected by the adsorption temperature i.e. higher temperatures lessen impurities adsorption due to the decrease in the equilibrium capacity of the molecular sieves as

temperature rises (Spath et al., 2005). Therefore, in this study design, the gas passes through series of heat exchangers to cool the gas down to 43°C prior to entering the PSA (stream 4). The tail gas containing (CO_2 = 10%, CO = 9%, CH_4 = 1%, N_2 = 6% and other hydrocarbon = 0.6%) from the PSA are reverted to the gasifier to be used as carrier gas.

(a)Hydrogen production: Hydrogen was compressed from 32 to 70 bars after the PSA (stream 5). A two-stage reciprocating compressor with an isentropic efficiency of 82% and interstage intercooler temperatures of 60°C each was used for the compression process.

(b)FT-Synthesis: The clean syngas with a correct ratio of H_2/CO (obtained by lowering a S/C ratio in the gasifier to 2.8) at a mass flow rate of 92398 kg/h enters a FT-reactor. A slurry phase FT reactor was selected for this study due to its simple configuration and its advantages in terms of good temperature control (Botes et al., 2013). A cobalt based catalyst was chosen as it is active at low temperature FTS and is commercially promoted for use in FTS due to it high selectivity to long chain hydrocarbons and olefins (Zhang et al., 2013). The FT-reactor was modelled using a RStoic reactor in which the fractional conversion is defined by a calculator block based on an estimated chain-length distribution. The product distribution follows the Anderson-Schulz-Flory alpha distribution which is represented in molar (M_n) or mass (W+) distribution variants (equations (6) and (7), (Song et al., 2004)). The chain growth factor (α) was established to be dependent on the partial pressures of H_2 and CO and temperature of the reactor for the cobalt based catalyst as shown in equation (8) (Song et al., 2004).

$$M_n = \alpha^{n-1}(1-\alpha) \quad (6)$$

$$W_n = \alpha^{n-1}(1-\alpha)^2 n \quad (7)$$

$$\alpha = \left[0.2332 \text{ x } \frac{Y_{CO}}{(Y_{CO}+Y_{H_2})} + 0.6330\right] \text{x } [1 - 0.0039 \text{ x } (T - 533)] \quad (8)$$

Where Y refers to the molar fraction of CO or H_2 and T (°C) refers to the reactor temperature.

The FTS was modelled to favour the production of diesel fuel. This was achieved by ajusting the α value within 0.85-0.9 (Swanson et al., 2010). The FT-reactor operated at 200°C and 25 bars, produces a chain growth factor of 0.88 with 95% syngas conversion and the FT-liquid containing 28wt% wax (paraffins at C_{30}) at a mass flow of 369427kg/h (stream 7). Therefore, the FT-liquid requires hydrocracking before it can be used as a fuel blend with fossil fuel. All effluents from the FT-reactor are cooled down to 30°C via heat exchangers. Water is separated from the hydrocarbons in a gas/liquid separator. The hydrocracker was operated at 400°C and 50 bars (Bezergianni and Kalogianni, 2009). The hydrocracking process was modelled with yields obtained from literature (Shah et al., 1988; Swanson et al., 2010) as shown in Table 3 with a 99% conversion of wax to hydrocarbons.

Table 3: Hydrocracking product distribution (Shah et al., 1988; Swanson et al., 2010)

Components	**Mass fraction**
Methane (CH_4)	0.035
LPG/Propane (C_3H_8)	0.088
Gasoline/Octane (C_8H_{18})	0.261
Diesel/Hexadecane ($C_{16}H_{34}$)	0.617

(c) Electricity production: Particulates, tar, sulphur compounds, nitrogen compounds and alkali metals can affect the performance of a gas turbine. Therefore, the gas is thoroughly cleaned before entering a gas turbine at a mass flow of 92398 kg/h (stream 9). The power generation process was simulated assuming a steady state conditions (Lan et al., 2018) . The syngas from the gasification unit is first cooled and compressed to recover the heat and then enters a combustion reactor. Air was supplied into the combustion reactor. The combusted gases expand in the gas turbine to generate power, which is then channelled to an electricity generator that converts the power to electricity ready to be sold. The main operating condition of the gas turbine can be found in supplementary material A.

3.2 Experiment and Modelling

Experimental analysis of the TSG of waste wood was conducted in a lab-scale at Newcastle University to understand how high volatile content lignocellulosic material in pyrolysis behaves. The study examine parameters (pyrolysis temperature, steam/carbon ratios, particle sizes and effect of gasifying environments) affecting the properties of char and volatiles (which are feedstock for gasification) so as to optimize operating conditions in pyrolysis for high quality syngas/hydrogen production (Prasertcharoensuk et al., 2019). Using data from previous studies (Prasertcharoensuk et al., 2019), an artificial neural network modelling was further conducted for optimising operating conditions of the TSG for high carbon conversion, high hydrogen yield and low CO_2 (Kargbo, H et al., 2021). The predicted conditions were then validated using experimental data. The predicted and experiment results agreed well in which the optimum operating conditions were 900˚C for the 1st stage and 1000^{o}C for the 2nd stage with a steam/carbon ratio of 3.8 to produce the gas yield of 96.2 wt%, hydrogen of 70 mol% and carbon dioxide of 16.4 mol% (Kargbo, H et al., 2021). The optimum operating conditions were then used in the Aspen Plus modelling for the hydrogen production (case 1). For cases 2 & 3, the same operating conditions were used except the steam/carbon ratio which was lowered to 2.8 to obtain a H_2/CO ratio close to 2.1 for the FTS. Table 4 shows the gas composition after gasification i.e., hydrogen

306 production (case 1), FTS (case 2) and electricity production (case 3) obtained from the lab-scale and
307 Aspen plus modelling of the TSG.

308 Table 4: Gas composition from a two-stage gasification experiment and modelling results

Operating condition and gas composition	**Experimental results for hydrogen production (case 1)**	**Aspen Plus modelling results**	
		Case 1: hydrogen production	**Cases 2 (liquid fuel) & 3 (electricity)**
1st stage temperature (pyrolysis) (˚C)	900	900	900
2nd stage temperature (gasification) (˚C)	1000	1000	1000
Gasifier pressure (bar)	1	1	1
Steam/carbon ratio	3.8	3.8	2.8
Gas compositions			
Gas yield (wt%)	96.5	97.7	96.6
CO_2 (mol%)	16.2	17.0	12.5
H_2 (mol%)	68.0	70.2	60.0
CH_4 (mol%)	3.4	2.3	2.4
CO (mol%)	9.0	9.6	25.0
Tar (g/m^3)	0.025	0.021	0.019
Solid residues (wt%)	0.5	0.3	0.6
NH_3	-	0.4	0.3
H_2S	-	0.1	0.1
H_2/CO ratio	7.6	7.3	2.4

309

310 The results from the modelling and experiment are in good agreement for case 1. Thus, the developed
311 Aspen Plus model is reliable to estimate the product yields at the outlet of the TSG. A very small

quantity of tar (0.025 g/m^3) together with a high H_2/CO ratio (2.4-7.6) was obtained. Therefore, the syngas in all three scenarios did not go through gas conditioning (steam reforming and shift reactions) and tar cracking. The small quantity of tar in the syngas was removed via cold-gas-cleaning technologies (wet scrubbing).

3.3 Plant power consumption

Power consumption in each section of the plant was estimated from Aspen Plus as presented in Table 5. It was assumed based on Spath et al. (2005)'s work that 90% of the plant power was produced via a steam cycle that produces steam through heat recovery of the hot process streams throughout the plant. The remaining 10% was purchased from the grid (for cases 1 and 2). However, this configuration (steam and power generation) was not modelled in this study, therefore the capital cost and other information for this process was based on information gathered from elsewhere (Spath et al., 2005; Swanson et al., 2010).

Table 5: Power consumption in all sections of the plant for each case study.

Electricity consumption (kW)	**Case1: Hydrogen**	**Case2: FT-liquid**	**Case3: Electricity**
Feed handling and drying	489	489	489
Two-stage gasification and quench	5261	5261	5261
Syngas cleaning and compression	14274	14282	13551
Hydrogen compression	3182		
FT synthesis and hydroprocessing		8631	
IGCC power generation			4546
Cooling water and other utilities	945	1111	943
Total plant electricity usage	**24151**	**29774**	**24790**
Electricity purchased from grid	**2415**	**2977**	**0**

The FTS path consumes the highest electricity among others due to the greater number of unit operations in the FTS plant compared to the hydrogen and electricity plants. From Table 5, the syngas cleaning and compression accounted for 57% of the total plant electricity consumption. This is due to the large number of processes occurring during gas cleaning i.e., several cyclones, filters, LOCAT adsorber, ZnO bed, PSA, compressors, and heat exchangers. The electricity produces annually on site for the case 3 is around 816 GWh in which only a small fraction, 24790 kW, was used to run the plant.

3.4 Economic analysis

3.4.1 Cost breakdown

The cost breakdown alongside total capital investment, total operating cost and minimum fuel selling price (MFSP) and levelized cost of electricity (LCOE) for the three cases are summarised in Table 6. Details of the calculations can be found in supplementary materials B (Table B5).

Table 6: Cost breakdown and MFSP/LCOE for all three cases (hydrogen, FT-liquid and electricity).

Economic variables	**Cost (million US $)**		
	Case 1 (hydrogen)	**Case 2 (FT-liquid)**	**Case 3 (electricity)**
Feed handling “and” drying	13.9	13.9	13.9
Two-stage gasification	22.2	22.2	22.2
Syngas clean-up “and” compression	28.5	28.6	26.0
Hydrogen compression	3.0		
Steam & power generation	15.6	17.6	12.1
Cooling water “and” other utilities	3.9	4.8	3.4
FT synthesis “and” hydroprocessing		53.0	
Gas turbine power generation			47.4
Total installed equipment cost	**87.2**	**140.1**	**124.4**
Fixed capital investment	186.8	300.4	266.9
Working capital	28.0	45.1	40.0
Total capital investment	**214.8**	**345.5**	**307.0**
Annualised capital cost (million US $/y)	**17.2**	**27.6**	**24.6**
	Cost (million US $/y)		
Fixed operating cost	12.6	25.1	22.5
Variable operating cost	18.6	28.9	20.3
Other direct operating costs (sales expense, general overheads, and R&D)	4.4	8.2	5.8
Total operating cost	**35.6**	**62.2**	**48.6**
Capacity ($x10^6$)	33 (kg /y)	0.081(m^3/y)	815 kWh/y
Capacity (GJ)	3971/y	3499/y	2934/y
MFSP (for cases 1 and 2) LCOE (for case 3)	**1.59 US $/kg**	**1,109 US $/$m^3$**	**0.09 US $/kWh**
MFSP, US $/GJ (for cases 1 and 2) LCOE, US $/GJ (for case 3)	**13000**	**26000**	**24000**

For comparison purposes, techno-economic analysis of biomass gasification using a single-stage fluidised bed gasifier (SSG) was also conducted to produce hydrogen, FT-liquid and electricity on the same basis as in the TSG. The resulting MFSP/LCOE of the SSG was shown in Figure 3 (details can be found in supplementary material A). The major difference between the two systems is the tar reforming and syngas conditioning processes (water-gas shift reactions and steam reforming of methane) in SSG, therefore increasing the capital and operating costs in the SSG. The MFSP of the SSG are around 25% (for the hydrogen and FT-liquid) and 10% (electricity case) higher than that of the TSG.

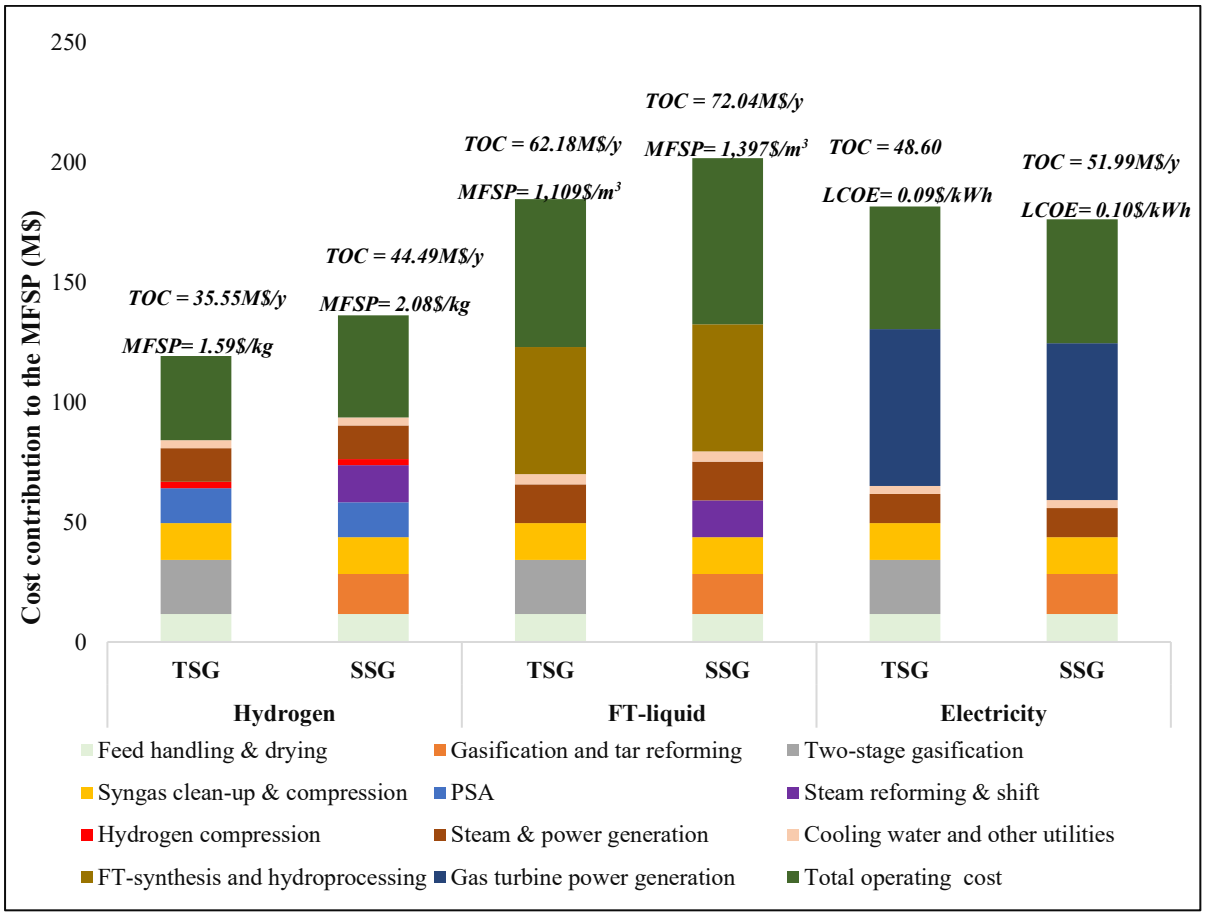

Figure 3: Economic comparison of the two-stage gasification (TSG) and single-stage gasification (SSG) systems for hydrogen, FT-liquid, and electricity production.

The difference in the total capital investment and operating cost among the three biofuel options is significant: FT-liquid and electricity production path requires almost 32% and 23% capital investment and 40% and 23% operating cost greater than the hydrogen production path. This difference is because of the additional unit operations required to convert syngas into FT- liquid or to electricity.

The MFSP for hydrogen (1.59 $/kg) obtained for the TSG system in this study is 50-75% lower than others using different reactor designs (3.2 $/kg of hydrogen from a dual fluidised bed gasification and 6.4 $/kg from sorption enhanced reforming of woody biomass) (Bioenergy, 2018). A typical H_2/CO

ratio of syngas from a dual fluidised bed system is between 1.6-1.8 and tar content is between 20-30 g/m^3(Bioenergy, 2018). Therefore, the syngas required shift reactions to increase the H_2 content in the producer gas and tar cracking or reforming whereas the TSG system produces a high H_2/CO ratio (~8) and a very small amount of tar (0.025 g/m^3), therefore a shift reactor or tar cracking process is not required. Although a sorption enhance reforming can produce syngas with a H_2/CO ratio of 9, the cost of solid waste disposal and high pressure application requires high electricity consumption and thus increase production cost (Bioenergy, 2018).

Considering other renewable hydrogen production technologies include solar power electrolyser (3.38-4.07 $/kg) (Yates et al., 2020), wind powered electrolyser (0.34-0-4.48 $/kg) (Gökçek, 2010), and coal gasification with carbon capture and storage (2.11–2.70 $/kg) (Olateju and Kumar, 2013), the TSG produces hydrogen at lower cost (MFSP of 1.59 $/kg), except for steam methane reforming of natural gas (about 1.19-1.25 $/kg at a natural gas price of 0.3 $/kg) (Basye and Swaminathan, 1997; Lemus and Duart, 2010). This can be due to the feedstock cost (assumed at 50$/tonne) used in this study, which contributes about 29-48% to the total operating cost. If the TSG is used for waste management, then the cost of feedstock is negligible while the plant will receive an additional gate fees of £20/t (Wrap, 2020), the TSG will produce hydrogen with the costs that comparable to hydrogen from steam methane reforming of natural gas. This is evidenced from the sensitivity analysis conducted in section 3.4.2. Also, the combination of feedstock flexibility (different feedstock sizes, relatively moist feedstock, high volatile content feedstock etc.) high fuel conversion, and technologies suitable for a wide range of scales are all technical advantages that mean two-gasification has fewer feedstock and technical constraints than other gasification technologies and thus suitable for waste management.

Techno-economic performance of SSG at scale of 1000-2000 t/d revealed that the production costs of FT-liquid from conventional SSG (using fixed bed, fluidised bed and entrained flow) are between 1,321-1,585$/m^3(4-6$/gge)(Kargbo, Hannah et al., 2021) depending on the economic assumptions, especially feedstock costs and scale of production. The average cost of fossil based liquid fuel (diesel and petrol) in the UK is approximately 1,672$/m^3(Report, 2021). The costs for FT liquid from TSG obtained in this study is lower (1,047$/m^3). However, this study excludes the cost of final distillation to the respective fuels (petrol and diesel). If the distillation cost (around 6% of the operating cost and 10% of the total capital investment (Zang et al., 2021)) is included, the MFSP is estimated to increase by 5-6% and therefore comparable to the current fossil fuel market price (1,672$/m^3).

The average cost for electricity from grid in the UK ranges between $0.17-0.18 per kWh. The TSG can produce electricity at almost half of that price (0.09$/kWh), excluding the cost of transmission to

individual homes and facilities (0.045$/kWh) (Administration, 2021). Thus, TSG of biomass offers an economically compelling case for hydrogen, FT-liquid, and electricity production.

3.4.2 Sensitivity Analyses

Sensitivity analyses were performed to evaluate the effect of different operating conditions (feedstock price, drying condition, and steam/carbon ratios) and their impacts on the MFSP as shown in Figure 4.

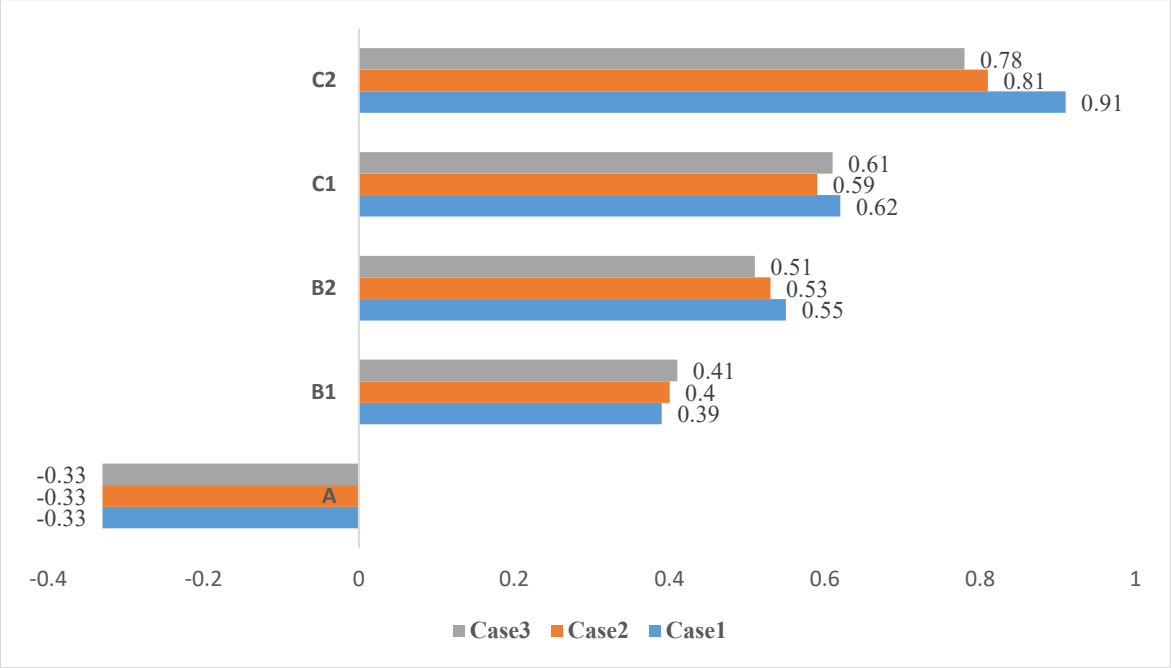

Figure 4: Sensitivity analyses showing A: feedstock price reduced to 30$/t B1: reducing drying of biomass feed to a moisture content of 30 wt% and maintained a constant gasifier temperature, B2: no drying, C1: increasing steam/carbon ratio to 6.5 and C2: decreasing the steam/carbon ratio to 1.5 for hydrogen production (case 1), FT-liquid (case 2) and electricity (case 3) production.

Feedstock cost contributes about 29-48% to the total operating costs. A 40% reduction in feedstock cost (A) leads to 18-20% reduction in the MFSP. However, a reduction of 40% in feedstock cost will only be feasible when waste and residues are used e.g. biomass waste in the UK in 2019 costs in a range from £5-10 per tonne (Wrap, 2019) . This cost is about 80% lower than the cost use in this study. On the other hand, if feedstock price continues to surge the only way out is an increase in the scale of production (larger plant size of around 2000 or more dry t/d) as evidence in Figure 5. Although drying contributes 8-13% of the total capital cost of the plant, removing drying step (C) leads to a 26% increase in MFSP (case1: hydrogen production), and about 18% increase in cases 2 (FT-liquid) and 3 (electricity). This is due to an increase in sizes of the gasifier and other related equipment and energy consumption to accommodate the amount of water content in the feedstock at a fixed plant capacity. An increase or decrease in the steam/carbon ratios (D &E) significantly affects the MFSP. Increasing a steam/carbon ratio from the base case (3.8 for case 1 and 2.8 for cases 2 & 3) to 6.5 increases the MFSP

411 by 17% due to the excess supply of steam promoting tar formation which in turn lowering the
412 hydrogen/syngas yield. On the other hand, at a low S/C ratio (1.5), a high percentage of methane and
413 solid carbon were produced, this lowers hydrogen and syngas ($CO + H_2$) yield, therefore increasing the
414 MFSP by 30%.

415 ***Effect of plant size on MFSP***

416 The plant size was varied for each case and its effect on the MFSP is presented in Figure 5. Increasing
417 the size of a plant decreases the MFSP particularly for hydrogen (case 1) and FT-liquid production (case
418 2). The MFSP for a plant size of 500 t/d doubles that to a plant of 1000 t/d (base case). When the plant
419 size increased to 2000 t/day, there was a 27-29 % reduction in the MFSP compared to the base case
420 (1000 t/d). Although the capital and operating costs increase as the plant size increases, the increased
421 costs are compensated by an increase in the output, which in turn lowers the MFSP. With a feedstock
422 cost of 50 US $/t (base case), the plant can be more profitable where there is a sustainably supply of
423 feed at a plant size of around 2000t/d. However, with larger plant sizes (2000t/d), there will be technical
424 challenges such as controlling operating parameters (temperature, pressure, and steam/carbon
425 ration) and optimising product yields. Moreover, pollution mitigation, waste management, biomass
426 supply, health and safety and storage of products in case of low demand are also challenging
427 particularly storing hydrogen. On the other hand, with a plant size less than 1000t/d, the cost of the
428 feedstock needs to reduce to 30-50% for the business to thrive well.

429

430

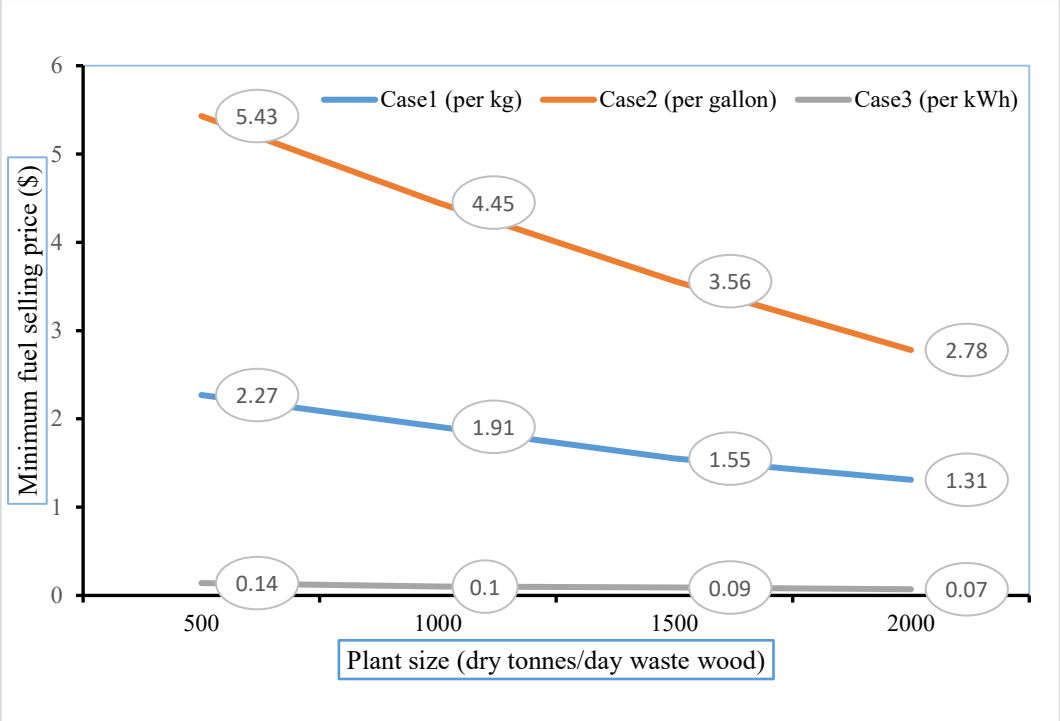

Figure 5: Effect of plant size on the minimum fuel selling price (MFSP)

4.0 Conclusions

A techno-economic analysis of a two-stage gasification (TSG) of biomass for hydrogen production, FT liquid production and electricity generation was conducted. With a capacity of 1000t/d of waste wood, the minimum selling price is 1.59$/kg hydrogen (compactable with "blue" hydrogen from natural gas reforming), 1,109$/m^3 FT-liquid (comparable to fossil-based fuels) and 0.09$/kWh electricity (around half the cost compared to electricity from grid in the UK). Using TSG can result in a 24-25% reduction in costs for the hydrogen and FT liquid, and 10% reduction for the electricity compared to single-stage gasification using fluidised bed gasifier. This is due to the reduction in capital and operating costs for cleaning and conditioning processes in TSG. The economics of the TSG can be further improved with reduced feedstock cost and large-scale plants.

Acknowledgement

The authors would like to thank the commonwealth commission in the UK for their financial support via PhD studentship (Scholarship reference number: LCS-2018-603) and EPSRC IAA . The authors would also like to thank Dr. Phuet Prasertcharoensuk for the laboratory analysis of the waste wood used as feedstock in this study.

Reference

Administration, U.S.E.I., 2021. Factors affecting electricity prices. https://www.eia.gov/energyexplained/electricity/prices-and-factors-affecting-prices.php. Access date: 12/07/2021

Anis, S., Zainal, Z., 2011. Tar reduction in biomass producer gas via mechanical, catalytic and thermal methods: A review. Renewable and sustainable energy reviews 15(5), 2355-2377.

Basye, L., Swaminathan, S., 1997. Hydrogen production costs--A survey. Sentech, Inc., Bethesda, MD (United States).

Bezergianni, S., Kalogianni, A., 2009. Hydrocracking of used cooking oil for biofuels production. Bioresource technology 100(17), 3927-3932.

Bioenergy, I., 2018. Hydrogen from biomass gasification. https://www.ieabioenergy.com/blog/publications/hydrogen-from-biomass-gasification/. Access date: 10/03/2021

Botes, F., Niemantsverdriet, J., Van De Loosdrecht, J., 2013. A comparison of cobalt and iron based slurry phase Fischer–Tropsch synthesis. Catalysis today 215, 112-120.

Broer, K.M., Peterson, C., 2019. Gasification. Thermochemical Processing of Biomass: Conversion into Fuels, Chemicals and Power, 85-123.

Cardoso, J., Silva, V., Eusébio, D., 2019. Techno-economic analysis of a biomass gasification power plant dealing with forestry residues blends for electricity production in Portugal. Journal of cleaner production 212, 741-753.

Chen, J., Xu, W., Zhang, F., Zuo, H., Jiaqiang, E., Wei, K., Liao, G., Fan, Y., 2019a. Thermodynamic and environmental analysis of integrated supercritical water gasification of coal for power and hydrogen production. Energy Conversion and Management 198, 111927.

Chen, J., Xu, W., Zuo, H., Wu, X., Jiaqiang, E., Wang, T., Zhang, F., Lu, N., 2019b. System development and environmental performance analysis of a solar-driven supercritical water gasification pilot plant for hydrogen production using life cycle assessment approach. Energy conversion and management 184, 60-73.

Dalena, F., Senatore, A., Marino, A., Gordano, A., Basile, M., Basile, A., 2018. Methanol production and applications: An overview, Methanol. Elsevier, pp. 3-28.

Department for Business, E.I.S., 2020. 2018 UK Greenhouse Gas Emissions,Final figures. https://assets.publishing.service.gov.uk/government/uploads/system/uploads/attachment_data/file/862887/2018_Final_greenhouse_gas_emissions_statistical_release.pdf. Access date: 12/11/2020.

Devi, L., Ptasinski, K.J., Janssen, F.J., 2003. A review of the primary measures for tar elimination in biomass gasification processes. Biomass and bioenergy 24(2), 125-140.

E4Tech, 2009. Review of Technologies for Gasification of Biomass and Wastes. https://www.ieabioenergy.com/wp-content/uploads/2021/02/Emerging-Gasification-Technologies_final.pdf. Access date: 06/09/2021.

EPA, 2020. Global Greenhouse Gas Emissions Data. https://www.epa.gov/ghgemissions/global-greenhouse-gas-emissions-data#:~:text=Global%20carbon%20emissions%20from%20fossil,increase%20from%201970%20to%202011. Access date: 26/11/2020

Garcia-Peréz, M., Garcia-Nunez, J.A., Pelaez-Samaniego, M.R., Kruger, C.E., Fuchs, M.R., Flora, G.E., 2020. Sustainability, business models, and techno-economic analysis of biomass pyrolysis technologies, Sustainable Business: Concepts, Methodologies, Tools, and Applications. IGI Global, pp. 1339-1373.

Gökçek, M., 2010. Hydrogen generation from small-scale wind-powered electrolysis system in different power matching modes. International Journal of Hydrogen Energy 35(19), 10050-10059.

Guo, F., Jia, X., Liang, S., Zhou, N., Chen, P., Ruan, R., 2020. Development of biochar-based nanocatalysts for tar cracking/reforming during biomass pyrolysis and gasification. Bioresource Technology 298, 122263.

Hai, I.U., Sher, F., Zarren, G., Liu, H., 2019. Experimental investigation of tar arresting techniques and their evaluation for product syngas cleaning from bubbling fluidized bed gasifier. Journal of Cleaner Production 240, 118239.

Harb, R., Rivera-Tinoco, R., Nemer, M., Zeghondy, B., Bouallou, C., 2020. Towards synthetic fuels production from biomass gasification: Tar content at low temperatures. Biomass and Bioenergy 137, 105540.

506 Henriksen, U., Ahrenfeldt, J., Jensen, T.K., Gøbel, B., Bentzen, J.D., Hindsgaul, C., Sørensen, L.H.,
507 2006. The design, construction and operation of a 75 kW two-stage gasifier. Energy 31(10-11), 1542-
508 1553.

509 Hu, W., Dang, Q., Rover, M., Brown, R.C., Wright, M.M., 2016. Comparative techno-economic
510 analysis of advanced biofuels, biochemicals, and hydrocarbon chemicals via the fast pyrolysis
511 platform. Biofuels 7(1), 57-67.

512 Jeong, Y.-S., Choi, Y.-K., Kang, B.-S., Ryu, J.-H., Kim, H.-S., Kang, M.-S., Ryu, L.-H., Kim, J.-S., 2020. Lab-
513 scale and pilot-scale two-stage gasification of biomass using active carbon for production of
514 hydrogen-rich and low-tar producer gas. Fuel Processing Technology 198, 106240.

515 Jones, K., 2015. Jhuma Sadhukhan, Kok Siew Ng and Elias Martinez Hernandez (Eds): Biorefineries
516 and Chemical Processes—Design, Integration and Sustainability Analysis. Springer.

517 Kargbo, H., Harris, J.S., Phan, A.N., 2021. "Drop-in" fuel production from biomass: Critical review on
518 techno-economic feasibility and sustainability. Renewable and Sustainable Energy Reviews 135,
519 110168.

520 Kargbo, H., Zhang, J., Phan, A.N., 2021. Optimisation of two-stage biomass gasification for hydrogen
521 production via artificial neural network. Applied Energy 302, 117567.

522 Kok Siew Ng, Sadhukhan, J., 2011. Techno-economic performance analysis of bio-oil based Fischer-
523 Tropsch and CHP synthesis platform. Biomass and Bioenergy 35(7), 3218-3234.

524 Ku, X., Wang, J., Jin, H., Lin, J., 2019. Effects of operating conditions and reactor structure on biomass
525 entrained-flow gasification. Renewable Energy 139, 781-795.

526 Kuo, P.-C., Illathukandy, B., Wu, W., Chang, J.-S., 2020. Plasma gasification performances of various
527 raw and torrefied biomass materials using different gasifying agents. Bioresource technology 314,
528 123740.

529 Lan, W., Chen, G., Zhu, X., Wang, X., Liu, C., Xu, B., 2018. Biomass gasification-gas turbine
530 combustion for power generation system model based on ASPEN PLUS. Science of the total
531 environment 628, 1278-1286.

532 Lemus, R.G., Duart, J.M.M., 2010. Updated hydrogen production costs and parities for conventional
533 and renewable technologies. International Journal of Hydrogen Energy 35(9), 3929-3936.

Lu, X., Cao, L., Wang, H., Peng, W., Xing, J., Wang, S., Cai, S., Shen, B., Yang, Q., Nielsen, C.P., 2019. Gasification of coal and biomass as a net carbon-negative power source for environment-friendly electricity generation in China. Proceedings of the National Academy of Sciences 116(17), 8206-8213.

Meng, J., Moore, A., Tilotta, D.C., Kelley, S.S., Adhikari, S., Park, S., 2015. Thermal and storage stability of bio-oil from pyrolysis of torrefied wood. Energy & Fuels 29(8), 5117-5126.

Ng, K.S., Martinez-Hernandez, E., 2020. Techno-economic assessment of an integrated bio-oil steam reforming and hydrodeoxygenation system for polygeneration of hydrogen, chemicals, and combined heat and power production, Towards Sustainable Chemical Processes. Elsevier, pp. 69-98.

Ng, K.S., Phan, A.N., 2021. Evaluating the techno-economic potential of an integrated material recovery and waste-to-hydrogen system. Resources, Conservation and Recycling 167, 105392.

Ng, K.S., Sadhukhan, J., Martinez-Hernandez, E., 2014. Biorefineries and Chemical Processes: Design, Integration and Sustainability Analysis.

Nielsen, R.G., Stoholm, P., Nielsen, M.B., Nørholm, N., Antonsen, S., Sander, B., Krogh, J., Henriksen, U.B., Qvale, E.B., 2005. The LT-CFB gasifier: First test results from the 500 kW test plant, 14th European Biomass Conference: Biomass for Energy, Industry and Climate Protection.

Olateju, B., Kumar, A., 2013. Techno-economic assessment of hydrogen production from underground coal gasification (UCG) in Western Canada with carbon capture and sequestration (CCS) for upgrading bitumen from oil sands. Applied Energy 111, 428-440.

Paethanom, A., Nakahara, S., Kobayashi, M., Prawisudha, P., Yoshikawa, K., 2012. Performance of tar removal by absorption and adsorption for biomass gasification. Fuel Processing Technology 104, 144-154.

Poškas, R., Sirvydas, A., Poškas, P., Jouhara, H., Striūgas, N., Pedišius, N., Valinčius, V., 2018. Investigation of warm gas clean-up of biofuel flue and producer gas using electrostatic precipitator. Energy 143, 943-949.

Prasertcharoensuk, P., Bull, S.J., Phan, A.N., 2019. Gasification of waste biomass for hydrogen production: Effects of pyrolysis parameters. Renewable Energy 143, 112-120.

561 Ramos, A., Berzosa, J., Espí, J., Clarens, F., Rouboa, A., 2020. Life cycle costing for plasma gasification
562 of municipal solid waste: A socio-economic approach. Energy Conversion and Management 209,
563 112508.

564 Rasmussen, N.B., Aryal, N., 2020. Syngas production using straw pellet gasification in fluidized bed
565 allothermal reactor under different temperature conditions. Fuel 263, 116706.

566 Ravenni, G., Elhami, O., Ahrenfeldt, J., Henriksen, U., Neubauer, Y., 2019. Adsorption and
567 decomposition of tar model compounds over the surface of gasification char and active carbon
568 within the temperature range 250–800° C. Applied energy 241, 139-151.

569 Report, A.F.P., 2021. UK and overseas petrol and diesel prices - June 2021.
570 https://www.theaa.com/driving-advice/driving-costs/fuel-prices. Access date: 12/07/2021

571 Riaza, J., Mason, P., Jones, J.M., Gibbins, J., Chalmers, H., 2019. High temperature volatile yield and
572 nitrogen partitioning during pyrolysis of coal and biomass fuels. Fuel 248, 215-220.

573 Rios, M.L.V., González, A.M., Lora, E.E.S., del Olmo, O.A.A., 2018. Reduction of tar generated during
574 biomass gasification: A review. Biomass and bioenergy 108, 345-370.

575 Sadhukhan, J., Ng, K.S., Hernandez, E.M., 2014. Biorefineries and chemical processes: design,
576 integration and sustainability analysis. John Wiley & Sons.

577 Saleem, F., Harris, J., Zhang, K., Harvey, A., 2019. Non-thermal plasma as a promising route for the
578 removal of tar from the product gas of biomass gasification-A critical review. Chemical Engineering
579 Journal, 122761.

580 Salkuyeh, Y.K., Saville, B.A., MacLean, H.L., 2017. Techno-economic analysis and life cycle assessment
581 of hydrogen production from natural gas using current and emerging technologies. International
582 Journal of hydrogen energy 42(30), 18894-18909.

583 Salkuyeh, Y.K., Saville, B.A., MacLean, H.L., 2018. Techno-economic analysis and life cycle assessment
584 of hydrogen production from different biomass gasification processes. International Journal of
585 Hydrogen Energy 43(20), 9514-9528.

586 Sara, H.R., Enrico, B., Mauro, V., Vincenzo, N., 2016. Techno-economic analysis of hydrogen
587 production using biomass gasification-A small scale power plant study. Energy Procedia 101, 806-
588 813.

589 Shah, P., Sturtevant, G., Gregor, J., Humbach, M., Padrta, F., Steigleder, K., 1988. Fischer-Tropsch
590 wax characterization and upgrading. UOP, Inc., Des Plaines, IL (USA); Allied-Signal, Inc., Des Plaines,
591 IL (USA ….

592 Shen, Y., Yoshikawa, K., 2013. Recent progresses in catalytic tar elimination during biomass
593 gasification or pyrolysis—A review. Renewable and Sustainable Energy Reviews 21, 371-392.

594 Simell, P., Hannula, I., Tuomi, S., Nieminen, M., Kurkela, E., Hiltunen, I., Kaisalo, N., Kihlman, J., 2014.
595 Clean syngas from biomass—process development and concept assessment. Biomass Conversion
596 and Biorefinery 4(4), 357-370.

597 Snehesh, A.S., Mukunda, H., Mahapatra, S., Dasappa, S., 2017. Fischer-Tropsch route for the
598 conversion of biomass to liquid fuels-Technical and economic analysis. Energy 130, 182-191.

599 Song, H.-S., Ramkrishna, D., Trinh, S., Wright, H., 2004. Operating strategies for Fischer-Tropsch
600 reactors: A model-directed study. Korean Journal of Chemical Engineering 21(2), 308-317.

601 Spath, P., Aden, A., Eggeman, T., Ringer, M., Wallace, B., Jechura, J., 2005. Biomass to hydrogen
602 production detailed design and economics utilizing the Battelle Columbus Laboratory indirectly-
603 heated gasifier. National Renewable Energy Lab., Golden, CO (US).

604 Swanson, R.M., Platon, A., Satrio, J., Brown, R., Hsu, D.D., 2010. Techno-economic analysis of
605 biofuels production based on gasification. National Renewable Energy Lab.(NREL), Golden, CO
606 (United States).

607 Swanson., R.M., Platon, A., Satrio, J.A., Brown, R.C., 2010. Techno-economic analysis of biomass-to-
608 liquids production based on gasification. Fuel 89, S11-S19.

609 Tan, R.S., Abdullah, T.A.T., Jalil, A.A., Isa, K.M., 2020. Optimization of hydrogen production from
610 steam reforming of biomass tar over Ni/dolomite/La2O3 catalysts. Journal of the Energy Institute
611 93(3), 1177-1186.

612 Wrap, 2019. Gate Fees report 2019. https://wrap.org.uk/resources/report/gate-fees-report-2019.
613 Access date: 03/11/2021.

614 Wrap, 2020. Gate Fees report 2020. https://wrap.org.uk/resources/report/gate-fees-report-2017.
615 Access date: 13/09/2021.

Yates, J., Daiyan, R., Patterson, R., Egan, R., Amal, R., Ho-Baille, A., Chang, N.L., 2020. Techno-economic analysis of hydrogen electrolysis from off-grid stand-alone photovoltaics incorporating uncertainty analysis. Cell Reports Physical Science 1(10), 100209.

Zang, G., Sun, P., Elgowainy, A.A., Bafana, A., Wang, M., 2021. Performance and cost analysis of liquid fuel production from H2 and CO2 based on the Fischer-Tropsch process. Journal of CO2 Utilization 46, 101459.

Zeng, J., Hu, J., Qiu, Y., Zhang, S., Zeng, D., Xiao, R., 2019. Multi-function of oxygen carrier for in-situ tar removal in chemical looping gasification: Naphthalene as a model compound. Applied Energy 253, 113502.

Zhang, Q., Chang, J., Wang, T., Xu, Y., 2007. Review of biomass pyrolysis oil properties and upgrading research. Energy conversion and management 48(1), 87-92.

Zhang, Q., Deng, W., Wang, Y., 2013. Recent advances in understanding the key catalyst factors for Fischer-Tropsch synthesis. Journal of Energy Chemistry 22(1), 27-38.

Zhao, X., Jiaqiang, E., Wu, G., Deng, Y., Han, D., Zhang, B., Zhang, Z., 2019. A review of studies using graphenes in energy conversion, energy storage and heat transfer development. Energy Conversion and Management 184, 581-599.

Zhao, X., Naqi, A., Walker, D.M., Roberge, T., Kastelic, M., Joseph, B., Kuhn, J.N., 2019. Correction: Conversion of landfill gas to liquid fuels through a TriFTS (tri-reforming and Fischer–Tropsch synthesis) process: a feasibility study. Sustainable Energy & Fuels.

Zheng, L., Furimsky, E., 2003. ASPEN simulation of cogeneration plants. Energy Conversion and Management 44(11), 1845-1851.

Zuo, H., Liu, G., Jiaqiang, E., Zuo, W., Wei, K., Hu, W., Tan, J., Zhong, D., 2019. Catastrophic analysis on the stability of a large dish solar thermal power generation system with wind-induced vibration. Solar Energy 183, 40-49.

Zuo, H., Tan, J., Wei, K., Huang, Z., Zhong, D., Xie, F., 2021. Effects of different poses and wind speeds on wind-induced vibration characteristics of a dish solar concentrator system. Renewable Energy 168, 1308-1326.